The colors seen behind transparent filters

Michael D'Zmura¶, Oliver Rinner, Karl R Gegenfurtner
Max-Planck-Institut für biologische Kybernetik, Spemanstrasse 38, D 72076 Tübingen, Germany
Received 27 September 1999, in revised form 28 June 2000

Abstract. How do the colors and lightnesses of surfaces seen to lie behind a transparent filter depend on the chromatic properties of the filter? A convergence model developed in prior work (D'Zmura et al, 1997 *Perception* **26** 471 – 492; Chen and D'Zmura, 1998 *Perception* **27** 595 – 608) suggests that the visual system interprets a filter's transformation of color in terms of a convergence in color space. Such a convergence is described by a color shift and a change in contrast. We tested the model using an asymmetric matching task. Observers adjusted, in computer graphic simulation, the color of a surface seen behind a transparent filter in order to match the color of a surface seen in plain view. The convergence model fits the color-matching results nearly as well as a more general affine-transformation model, even though the latter has many more parameters. Other models, including von Kries scaling, did not perform as well. These results suggest that the color constancy revealed in this task is described best by a model that takes into account both color shifts and changes in contrast.

1 Introduction

In recent work (D'Zmura et al 1997), we presented a convergence model for the perception of color transparency that is based on earlier work by Metelli (1974), Beck (1978), Da Pos (1989), Gerbino et al (1990), and others. The model predicts that an area of the visual field will appear transparent if the colors of lights from surfaces along the border of that area converge towards some point in color space as the surfaces pass from outside the area to within. The model is based on observations which suggest that shift in color and change in contrast lead effectively to the perception of transparency, but that rotation and shear in color space do not. Color shifts and contrast changes are captured by the convergence model, whose four parameters include three that describe the color shift and one that describes the change in contrast.

We tested the model psychophysically in further work (Chen and D'Zmura 1998). A display with four colored regions was used; the colors of three of the regions were chosen in advance by the experimenter. The observer set the color of the fourth region so that a central square area would appear transparent. Observers' settings agreed well with the predictions of the convergence model, which is that settings for the fourth region lie along a line segment in color space determined by the chromatic properties of the other three regions. This result is similar to one reported by Faul (1997).

In this paper, we examine whether the convergence model describes the color appearance of surfaces seen to lie behind transparent filters. We use an asymmetric color-matching technique to measure surface color. With this technique, one matches the color of a surface viewed under a test condition to the color of a surface viewed under a reference condition (Wyszecki and Stiles 1982). In this work, we compare the chromatic properties of test surfaces seen to lie behind a transparent filter to the properties of reference surfaces seen in plain view. The comparison reveals the effects of the transparent filter on judgments of surface color. In particular, the comparison shows how well observers discount the chromatic properties of the transparent filter when judging surface color.

¶ Address for correspondence: Department of Cognitive Sciences, University of California at Irvine, Irvine, CA 92697, USA; e-mail: mdzmura@uci.edu

The convergence model fits the color-matching results very well. The convergence model has three parameters that describe a change in color, similar to models of color constancy that rely on von Kries adaptation (von Kries 1905; Brainard and Wandell 1992; Foster and Nascimento 1994; Bäuml 1999). The convergence model has a fourth parameter that takes into account changes in contrast. The contrast parameter distinguishes the present model of color constancy from the earlier ones. It is also required to fit the data reported in this paper. A preliminary report of this work was made by D'Zmura et al (1998).

2 Methods
Observers viewed an array of colored squares, atop which a transparent filter appeared to drift back and forth. With this display, they performed an asymmetric matching task, in which the color of a test square that appeared behind the filter was adjusted to match the color of an unobscured reference square.

2.1 Display
The stimuli were presented on a Sony Trinitron GDM 20D11 color monitor, which observers viewed binocularly at a distance of 70 cm in a dark room. Software on a Silicon Graphics Indigo R4000 computer provided 24 bits of chromatic information for each of the 1280×1024 pixels presented on the monitor at a field rate of 72 Hz (non-interlaced). The nonlinear relationship between applied voltage and phosphor intensity was corrected, for each gun, with the aid of color lookup tables. The chromaticities and luminances of the three phosphors of the monitor were measured with a PhotoResearch PR750 spectroradiometer. The CIE 1931 standard-observer chromaticities and maximal luminances are presented in table 1. The background area of the display was set to black.

Table 1. CIE 1931 standard observer chromaticity (x, y) and maximal luminance L_{max} of each phosphor R, G, and B.

	R	G	B
x	0.623	0.280	0.150
y	0.343	0.605	0.063
L_{max} /cd m^{-2}	11.2	38.4	4.78

2.2 Spatial configuration
The stimulus was centered on the face of the monitor and subtended 20 cm $\times$ 20 cm or 16.2 deg $\times$ 16.2 deg of visual angle. The stimulus comprised 7×7 or 49 areas, each of uniform color and approximately in the shape of a square of size 2.3 deg $\times$ 2.3 deg (see figure 1). These pseudosquares were generated by, first, perturbing square size randomly by adding independent increments to both height and width drawn from distributions uniform on the interval [0, 0.37] deg and, second, drawing these squares in random order into the computer image frame buffer, so that through occlusion cues some pseudosquares would appear to lie in front of others. The square shapes were perturbed in this fashion to avoid undesired instances of transparency that arise when squares in uniform square arrays are colored randomly.

Pseudosquare chromatic properties were modulated in a way to produce the impression of a transparent filter within a central square area with a side length 2.5 times that of the small pseudosquares, ie of size 5.7 deg $\times$ 5.7 deg (see figure 1). The simulated filter drifted from left to right and back again at constant speed. A single cycle of oscillation had a duration of 0.9375 s, so that the rate of oscillation was 1.067 Hz. The maximum excursion of the filter about its central position to the left and to the right was 1.5 deg. The task of observers was either to judge or to adjust the
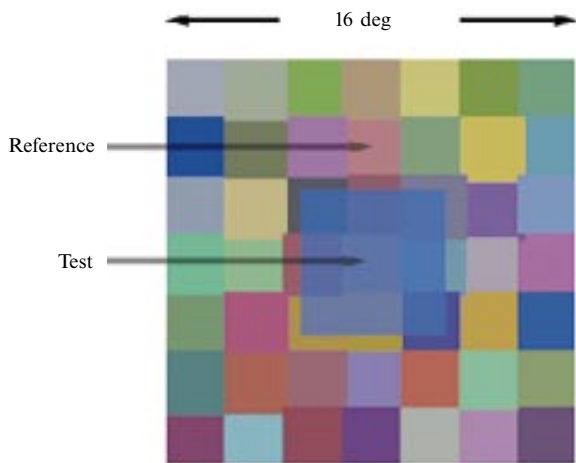
Figure 1. Stimulus configuration; see text for details. [This figure and figure 3 are also available on our website under www.perceptionweb.com/perc0800/dzmura.html and will be archived on the annual CD-ROM sent with issue 12 of the journal.]

chromatic properties of the central pseudosquare that lay in the fourth column and in the fourth row. This central test area was covered at all times by the simulated filter.

The movement of the simulated filter back and forth across the central area of the display helped observers to maintain a clear sense of the filter's presence. A static filter would often appear to blend into the simulated surfaces. Without filter movement, observers would lose the perception of surface – filter separation required for the present investigation.

2.3 Color space

The color properties of stimuli are described in the DKL color space (Derrington et al 1984), which is based on the MacLeod and Boynton (1979) color diagram. Features in this color space, shown in figure 2, are defined relative to the neutral gray point G, which serves in these experiments as the expected color of the 49 pseudosquares when seen in plain view. The gray point G was set to the light created by displaying simultaneously each of the monitor's phosphors at half-maximal intensity. The chromaticity of G was (0.28, 0.30), and its luminance was 27.2 cd m^{-2}.

The color space is defined by three axes which intersect at the gray point G. The first is the achromatic axis (A), lights along which are created by generating equal modulations of the three phosphors about G and differ in brightness. The other two axes lie in the equiluminous plane through G; all lights in this plane are of equal luminance as defined by the V_λ photopic luminosity function (Wyszecki and Stiles 1982). Modulation along the L&M (LM) axis changes the excitations of the long-wavelength-sensitive (L) and medium-wavelength-sensitive (M) cones and is invisible to the short-wavelength-sensitive (S) cones. Lights along this axis typically appear red
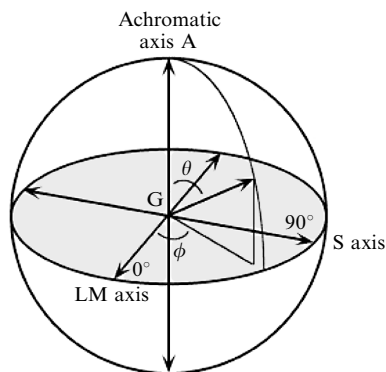

Figure 2. Color space; see text for details.

or blue – green. Modulation along the S axis changes the excitation of S cones and is invisible to L and M cones. Lights along this axis typically appear yellow – green or purple.

The direction of a half-axis that emanates from the gray point G can be described in terms of spherical coordinates (see figure 2). The elevation θ is defined to be the angle between the half-axis and the 'white' end of the achromatic axis. Axes in the equiluminous plane have an elevation of 90°; the 'black' end of the achromatic axis has an elevation of 180°. The azimuth ϕ is defined to be the angle between the projection of the half-axis onto the equiluminous plane and the 'red' end of the LM axis (Derrington et al 1984).

One can specify the length of a vector which lies along a particular half-axis in terms of the contrast delivered to the cone mechanisms (Smith and Pokorny 1975). The maximum value of contrast that could be provided to S-cones by modulating lights about the gray point G along the S axis was 0.91, while the maximum amount of contrast that we could provide to L cones by modulating lights about G along the LM axis was 0.082.

2.4 *Chromatic properties*

Simulated surfaces seen in plain view had RGB values that were drawn randomly from a parallelepiped in color space (see figure 1). Half-maximal positive and negative modulations of the intensity of a single phosphor about the gray point G defined an interval, for that phosphor, from which a value was drawn according to a uniform distribution. For each surface—other than the reference and test surfaces—such a random draw was performed independently for each of the three phosphors to provide the surface chromatic stimulus.

The effects of a simulated filter on surface chromatic properties were specified with the convergence model (Da Pos 1989; Faul 1997; D'Zmura et al 1997; Chen and D'Zmura 1998). The intuition behind the model is that the effects of a transparent overlay may be captured by two color processes, the first a shift in color and the second a change in contrast. A cloudy yellow filter, for instance, causes the colors of underlying surfaces to become yellower (a shift in color) and also cloudier (reduction in contrast). To formulate this model, suppose that the chromatic properties of the light from a surface seen in plain view are represented by the three-dimensional vector $\boldsymbol{a}$ and that the target of convergence is represented by vector $\boldsymbol{s}$. Then the light from the surface is shifted from $\boldsymbol{a}$ to $\boldsymbol{s}$ by an amount α to produce the color vector $\boldsymbol{b}$ of the light seen through the transparent overlay:

$$\boldsymbol{b} = (1 - \alpha)\boldsymbol{a} + \alpha\boldsymbol{s} . \tag{1a}$$

The parameter α determines how much contrast is reduced towards the target of convergence $\boldsymbol{s}$. If the target of convergence is located at an infinite distance, then the convergence degenerates into a simple, parallel shift. An equivalent formulation sets the parameter β equal to $1 - \alpha$ and creates the translation $\boldsymbol{t}$ from the product $\alpha\boldsymbol{s}$:

$$\boldsymbol{b} = \beta\boldsymbol{a} + \boldsymbol{t} . \tag{1b}$$

These formulations of convergence are identical to those used in computer graphics to simulate transparency (Foley et al 1990).

2.5 *Conditions*

In a first set of conditions, observers matched colors of surfaces seen through 24 filters with targets of convergence that were equal in luminance to the gray point G. In this 'color' set of conditions, the 17 reference colors were also equal in luminance to the gray point. The chromatic properties of the 17 reference colors are listed in table 2. In a second set of conditions, observers matched colors of surfaces seen through 18 filters with targets of convergence that varied in luminance. In this 'lightness' set of conditions, 15 reference colors were used that varied in luminance; their chromatic properties are listed in table 3.

Table 2. CIE 1931 standard observer (x, y) chromaticities of the 17 reference colors in the color conditions. Their luminance was 27.2 cd m^{-2}.

x	0.275	0.287	0.298	0.294	0.316	0.288	0.304	0.283	0.292
y	0.296	0.291	0.287	0.320	0.349	0.322	0.355	0.325	0.361
x	0.263	0.251	0.260	0.246	0.264	0.255	0.269	0.264	
y	0.300	0.305	0.275	0.257	0.273	0.254	0.271	0.251	

Table 3. CIE 1931 standard observer (x, y) chromaticities and luminances of the 15 reference colors in the lightness conditions.

x	0.275	0.275	0.284	0.298	0.300	0.275	0.267	0.251
y	0.296	0.296	0.292	0.287	0.286	0.296	0.299	0.305
L/cd m^{-2}	27.2	40.8	40.8	27.2	13.6	13.6	40.8	27.2
x	0.249	0.300	0.313	0.321	0.258	0.251	0.248	
y	0.306	0.347	0.374	0.390	0.259	0.246	0.240	
L/cd m^{-2}	13.6	33.6	27.2	20.0	33.6	27.2	20.0	

2.5.1 *Color conditions.* For each of the four cardinal half-axes in the equiluminous plane, six filters were chosen that varied in saturation of convergence target and in the contrast parameter α, for a total of 24 filters. The four cardinal half-axes are +LM (red, azimuth 0°), −LM (blue – green, azimuth 180°), +S (purple, azimuth 270°), and −S (yellow – green, azimuth 90°).

The levels of saturation and contrast parameter along each half-axis are illustrated in figure 3 for the blue – green filters along the −LM half-axis. The left column of figure 3 shows filters with targets of convergence that have one-half the saturation of the filters in the right column. The contrast provided to the L cones by the target of convergence of the filters illustrated at right, computed relative to the gray point G, was −0.022, while that provided by the targets at left was −0.011. The contrasts provided to the L cones by the red targets of convergence along the +LM half-axis had the opposite sign. The contrast provided to the S cones by the fully saturated targets of convergence along the +S half-axis was 0.45. That to the targets of half-saturation was 0.23. The sign of the contrast was reversed for filters along the −S half-axis.

The filters with half-saturated targets (figure 3, left column) had contrast-reduction parameters α set to either 0.0 (above) or 0.5 (below). The filters with fully saturated targets (figure 3, right column) had contrast-reduction parameters set to 0.0 (top), 0.25 (second from top), 0.5 (third from top), or 0.75 (bottom). One sees that as the parameter α increases in value, the filter becomes less clear and more clouded in appearance.

2.5.2 *Lightness conditions.* Further filter axes and reference colors that combined changes in lightness and color were investigated. For each of three half-axes +LM (red, elevation 90°), +LM − A (dark red, elevation 110°), and −A (dark gray, elevation 180°), six filters were chosen and 15 reference colors were used which spanned the three dimensions of color space. The six filters used in the +LM (red) lightness conditions were identical to the red filters used in the color conditions.

The achromatic contrast provided by the target of convergence of the dark-red filters was 0.17 for the two low-contrast conditions and was 0.34 for the four high-contrast conditions. The achromatic contrast of the target of convergence of the dark-gray filters was either 0.25 or 0.5. The contrast-reduction parameters of the filters used in the dark-red and dark-gray conditions varied like those in the color conditions.
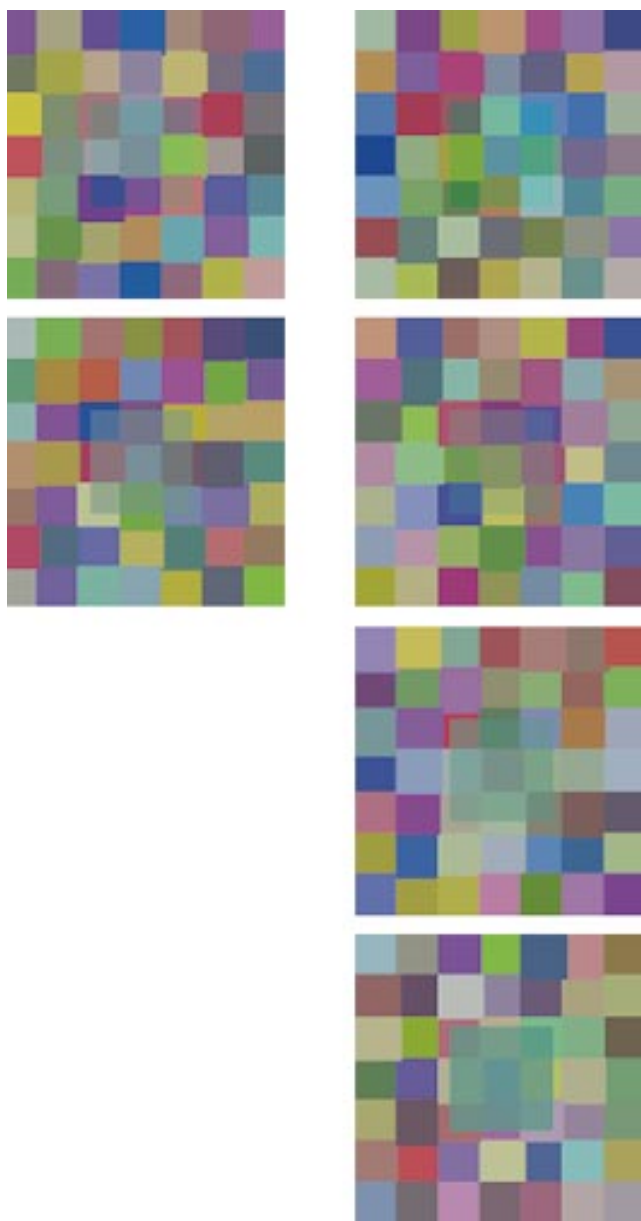
Figure 3. Examples of filters used in the color conditions. For each of four cardinal color half-axes in the isoluminous plane, six filters were chosen that varied in the saturation of their target and in the amount of contrast reduction. Six filters along the blue – green end of the LM axis are pictured here. The total number of color conditions was 24 (six filters for each of four half-axes). See text for further details.

2.6 *Observers*

Observers matched 17 reference colors arrayed about the neutral gray point for each of the 24 color conditions and 15 reference colors for each of the 18 lightness conditions. Settings for each reference color in the color conditions, for each filter, were made by each of three color-normal observers, two of whom (OR and MD) are authors. These two observers made the settings in the lightness conditions. All three observers made five repeated measurements of color matches in the single-color condition plotted in figure 4.
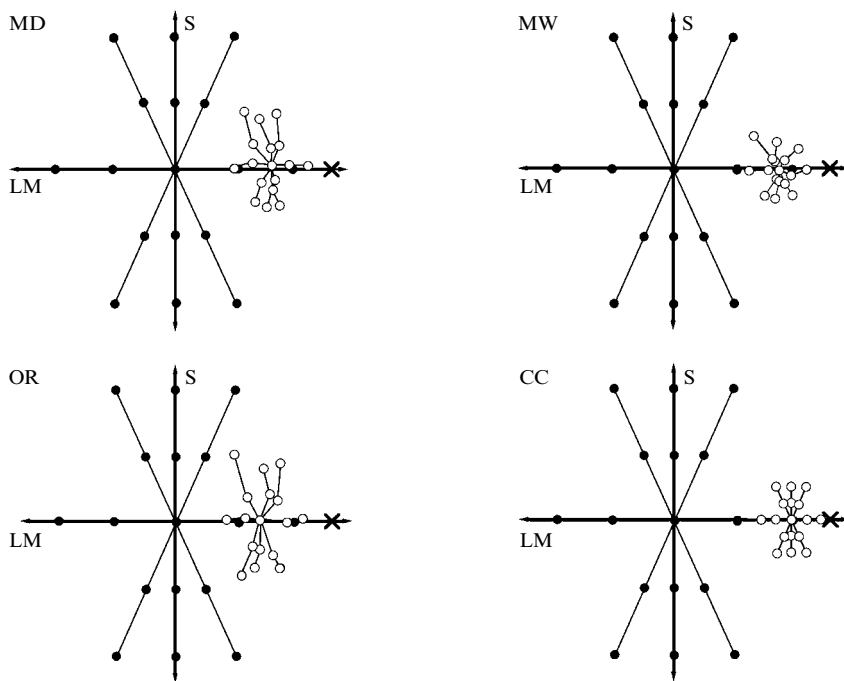
Figure 4. Results of color-matching for a red filter with target of convergence marked by ✕. Reference colors and observer settings are indicated in the equiluminous plane by the filled and unfilled circles, respectively. Results are shown for observers MD, OR, and MW; bottom right: perfectly color constant (CC) settings.

Observers were instructed to match surface color appearance; they adjusted the chromatic properties of the central test square so that it appeared to be made of the same material as the reference square. Observers used the keyboard to adjust test-square appearance; six keys on the computer keyboard were arranged in three pairs to control change along the A, LM, and S axes in the DKL color space, respectively.

Observers repeated trials in just a single-color condition. The three observers repeated five times the 17 color matches made in a condition with a red filter described in detail in the following section; results from this condition are shown in figure 4.

3 Results
We collected color-matching data as a function of the chromatic properties of the transparent filter and as a function of reference color. Numerous models were used to fit the data. Results show that the convergence model, with four parameters, fits the data nearly as well as the twelve-parameter affine model. Comparing the fit parameters of the convergence model to the filter parameters shows that the contrast-reduction parameter α is essential in fitting the data. The comparison also provides an estimate of how much color constancy is exhibited by observers in these tasks.

3.1 *Results for a red filter*
Panels of figure 4 marked MD, OR, and MW show results for the three observers in the repeated-trials condition with a high-saturation target of convergence (marked ✕) along the 'red' end of the LM axis and a value of 0.75 for the transparency parameter α. The reference colors lie in the equiluminous plane spanned by the LM and S axes; these colors are shown by the filled circles. The open circles show averages of observers' five settings.

3.1.1 *Color shift and contrast reduction.* A simple translation of the reference colors towards the 'red' end of the LM axis does not describe the data shown for the three observers in figure 4. Likewise, a simple convergence of the reference colors towards the neutral gray at the center of the diagram is inadequate. Simultaneous color shift and contrast reduction are required to help understand perceived surface color.

Were the observers to take into account fully the chromatic transformation caused by the red filter, then their settings would be like those marked in the CC panel of figure 4. These 'color constant' settings lie three-quarters of the way along the line segments that join the corresponding reference color points to the point labeled ✕ that marks the target of convergence. Observers are only partially color-constant; we quantify the degree of constancy in observers' settings below after an exposition of models fit to the data.

3.1.2 *Reliability.* One can quantify the reliability of these repeated settings by computing, for each reference color, the distance in color space between the average setting (shown by the filled circle) and the five settings that contribute to the average setting. One can then find a measure of reliability for each observer by averaging these distances across the 17 reference colors.

We measure distance in the DKL color space, scaled in a manner so that one unit along achromatic, LM, or S axes corresponds approximately to threshold. The achromatic axis of the DKL color space was scaled by using an achromatic contrast sensitivity of 200, which corresponds to a (reciprocal) threshold contrast of 0.005 for the achromatic axis. A contrast sensitivity to L cones of 1000 was used to scale the LM axis; this sensitivity corresponds to a threshold contrast of 0.001 to L cones. For the S axis, we used a contrast sensitivity of 100 to S cones, which corresponds to a threshold contrast of 0.01 (Lennie and D'Zmura 1988). These contrasts are computed relative to the gray point G.

The average distance between settings and their averages was for observer MW 4.72, for observer OR 3.55, and for observer MD 3.48 in DKL threshold units. This means that the average distance of a particular setting from an average (displayed by the open symbols in figure 4) was approximately 4.7 times threshold for observer MW and 3.5 times threshold for observers OR and MD.

3.2 *Models*

We fit the data from the 42 conditions in eleven different ways. Six models were applied in the DKL color space (Derrington et al 1984), and five models were applied in the space of *LMS* cone excitations (Smith and Pokorny 1975). Models applied in the DKL space include the affine, convergence, general convergence, linear, diagonal, and translation models. Models applied in the *LMS* cone excitation space include the affine, convergence, linear, translation, and von Kries scaling models. The models are described in detail below. The PRAXIS fitting procedure (Gegenfurtner 1992) was used to minimize the root-mean-squared (rms) error between model predictions and the observers' actual settings.

In fitting the models, the DKL space was scaled so that one unit along achromatic, LM, and S axes corresponded approximately to the respective contrast thresholds when the scaling described in section 3.1.2 was used. The fits of models in the *LMS* space are converted to the threshold-scaled DKL space to provide a uniform basis for comparison for all models, whether applied in the DKL space or the *LMS* space.

3.2.1 *Affine model.* The affine model is described by the equation

$$b = Ma + t, \tag{2}$$

in which a is a three-dimensional vector of reference-color coordinates, M is a 3×3 matrix that describes a linear transformation, t is a three-dimensional translation vector,

and **b** is a predicted vector of test-color coordinates. In fitting the model to the color-matching data found by an observer in a particular condition, one chooses the entries of the matrix **M** and the vector **t** so as to minimize the rms error between the predictions and an observer's actual settings. The affine model has 12 parameters that may be adjusted during the fitting procedure: nine for the 3×3 linear transformation **M** and three for the color shift **t**. We applied this model in both the DKL color space and in the *LMS* space of cone excitations.

Note that the DKL space itself represents an affine transformation of the *LMS* space. Cone excitations are transformed into DKL color coordinates by, first, subtracting from the cone excitations the excitations of the gray point G and, second, transforming the differences linearly to produce DKL color coordinates (Derrington et al 1984). One consequence of this relationship between the two spaces is that the parameters of the best-fit affine model in *LMS* space are identical to those of the best-fit affine model in DKL space.

3.2.2 *Convergence model.* The convergence model is described by equation (1). It has only four parameters: three for describing a color shift and one for describing change of contrast. This model is a special case of the affine model described in the previous section; the parameter which describes change of contrast can be thought of as providing the three on-diagonal entries of a diagonal matrix that acts on the reference-color vector **a**.

3.2.3 *General convergence model.* The general convergence model has six parameters: three for describing a color shift and three for describing change of contrast. It is given by the following equation:

$$b = \mathbf{D}a + t. \tag{3}$$

The 3×3 matrix **D** is a diagonal matrix with three non-zero elements along the diagonal. These elements may be used to describe change of contrast uniquely along each of the three axes in color space. The convergence model of section 3.2.2 is a special case of the general convergence model which, in turn, is a special case of the affine model.

3.2.4 *Linear model.* The linear model is also a special case of the affine model. It has nine parameters that describe a 3×3 linear transformation and is defined by the following equation:

$$b = \mathbf{M}a. \tag{4}$$

This model has nine parameters and lacks the translation **t** of the affine and convergence models.

3.2.5 *Diagonal model.* We call the model in which DKL color coordinates are transformed by means of a diagonal matrix the diagonal model. It can be expressed by the equation

$$b = \mathbf{D}a, \tag{5}$$

in which **a** is a vector of reference DKL color coordinates and **D** is a diagonal matrix that scales DKL coordinates to produce the scaled DKL coordinates **b**. The same transformation, when applied to *LMS* cone excitations, corresponds to the von Kries scaling model (see section 3.2.7 below).

3.2.6 *Translation model.* Also a special case of the affine model, the translation model has three parameters and is described by

$$b = a + t. \tag{6}$$

This model has no contrast-reduction parameter. Comparing the fits of this model to the fits by the convergence model will be one way to assess the importance of the contrast-reduction parameter α to the modeling of these color constancy data.

3.2.7 *Von Kries scaling model.* The von Kries scaling model can be expressed by the equation

$$b = \mathbf{D}a, \tag{7}$$

in which a is a vector of reference color L, M, and S cone excitations, and $\mathbf{D}$ is a diagonal matrix that acts to scale the cone excitations to produce the scaled cone excitations b predicted by the model. To fit data with this model, we first convert color specifications from the DKL space to the *LMS* space of cone excitations. There we fit the data using three factors to scale the respective cone excitations. We then convert the results from the *LMS* space back to the DKL space so that they may be compared with the fits of the other models. The conversion of fits from *LMS* to DKL space is performed with all models employed in the *LMS* space of cone excitations; all fits are evaluated in the threshold-scaled DKL space to provide a uniform basis for comparison.

3.3 Model fits
3.3.1 *Fits to color condition data.* Figure 5 shows the average of the residual mean squared errors for observers MW, OR, and MD in the color conditions: (a) the results found when fitting models in the DKL color space, and (b) results found when fitting models in the *LMS* space of cone excitations. In (a), the correspondence between letters and models is as follows: A—affine, C—convergence, GC—general convergence, L—linear, D—diagonal, and T—translation. In (b), the correspondence is A—affine, C—convergence, L—linear, T—translation, and S—von Kries scaling. A better fit corresponds to a smaller value.
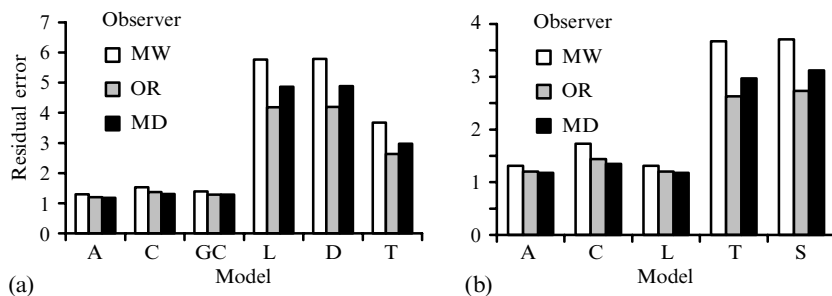

Figure 5. Model fits for the color conditions, by observer. (a) Fits in the DKL color space. (b) Fits in the space of *LMS* cone excitations. Each column lists the average of residual mean squared errors found in fitting a model to each of the 24 color conditions. The model is listed by its first letter along the horizontal axis. The models in (a), for the fits in DKL color space, are referred to by the letters A for affine, C for convergence, GC for general convergence, L for linear, D for diagonal, and T for translation. The models in (b), for the fits in the *LMS* space of cone excitations, are referred to by letters A for affine, C for convergence, L for linear, T for translation, and S for von Kries scaling. Residual variances found for observers MW, OR, and MD with the identity transformation used as a model were 180.5, 84.3, and 115.1, respectively.

The affine model (leftmost columns) fits the data best for all three observers, in both the DKL and the *LMS* color spaces. This holds true for all of the analyses that we have performed. Indeed, the affine model must perform at least as well as the other models, because they are all special cases of the affine model.

The results of fits in the DKL color space (figure 5a) show that the convergence model fits the data nearly as well as do the general convergence and affine models; and that the linear, diagonal, and translation models perform less well. Similar results are found with the fits in the *LMS* space of cone excitations (figure 5b). The convergence model

fits the data nearly as well as do the affine and linear models in *LMS* space, and the translation and von Kries scaling models perform less well.

One can judge the absolute quality of a model fit by comparing its residual variance to that found on using the identity transformation as a model. The variances found for observers MW, OR, and MD in the color conditions with the identity transformation used as a model were 180.5, 84.3, and 115.1, respectively. The amounts of variance accounted for by a particular model in one or the other color space can be found by comparing the values plotted in the appropriate set of columns to these identity transformation residuals. For instance, the amounts of variance accounted for by the convergence model applied in the *LMS* space can be found by comparing the values plotted in the second set of columns (labeled C) in figure 5a to the identity transformation residuals. The amounts of variance accounted for in this example are thus $(180.5 - 1.73)/180.5 = 99.0\%$, $(84.3 - 1.44)/84.3 = 98.3\%$, and $(115.1 - 1.35)/115.1 = 98.8\%$, for MW, OR, and MD, respectively, in the 24 color conditions. Identity transformation residuals are specified in figure captions.

We used the convergence model to fit the data from the experiment with a red filter (section 3.1) in which observers made repeated settings, in a further attempt to assess the quality of the fits. The best model fits had an average deviation about 10% higher than the reliability of the repeated settings. Individual values were 3.6% (MW), 10.8% (OR), and 11.6% (MD). These values show that the quality of the best model fits was high, with deviations comparable to those associated with trial-to-trial variability.

An implication of the similarity in the abilities of the affine and convergence models to fit the data is that the eight extra degrees of freedom within the linear transformation of the affine model do not account for much variance in the data beyond that accounted for by the contrast-reduction parameter. This conclusion is bolstered by the values in figure 6, which show the residual errors in the model fits as a function of filter contrast-reduction parameter α. The expectation that the contrast-reduction parameter of the convergence model gains in importance as filter α increases is borne out by the numbers. In the DKL color space (figure 6a), the residual error of the convergence model for filters with α equal to 0.0 is 1.95, but is reduced to 1.05 when α is equal to 0.75. One also finds, in accordance with expectation, that the fit of the translation model becomes increasingly poor as filter contrast reduction increases. The residual error of the translation model increases from 2.38 to 4.51 as α is increased from zero to 0.75. These trends are also found for the fits in *LMS* cone excitation space (figure 6b). The residual error of the convergence model in the *LMS* space decreases from 2.09 to 1.05 as α increases. Yet the fits of the linear, translation, and von Kries scaling models grow increasingly poor as filter cloudiness increases.
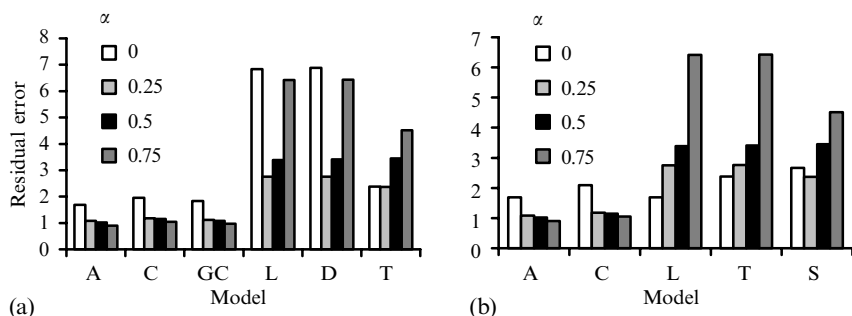

(a)   (b)

Figure 6. Model fits for matches in the color conditions, as a function of filter contrast-reduction parameter α. (a) Fits in the DKL color space. (b) Fits in the space of *LMS* cone excitations. Models are labeled as in figure 5. Residual variances found for contrast reductions 0, 0.25, 0.5, and 0.75 with the identity transformation used as a model were 164.9, 44.4, 88.7, and 208.1, respectively.

Figure 7 shows the residual mean squared errors as a function of the color of filter target of convergence. These results show that the quality of the fits provided by the convergence model does not depend in any substantial way on filter hue.
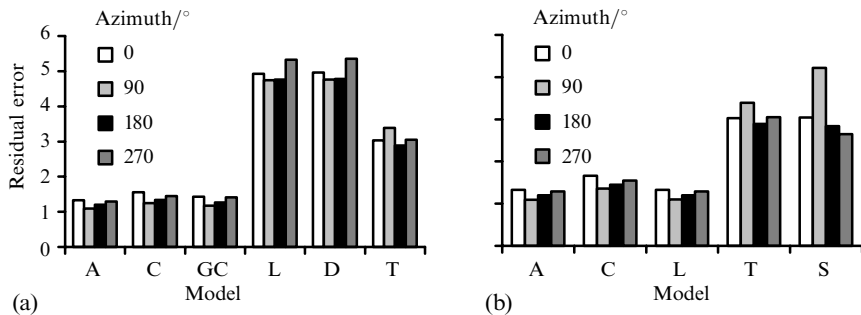

Figure 7. Model fits by filter color azimuth for the color conditions. (a) Fits in the DKL color space. (b) Fits in the space of *LMS* cone excitations. Models are labeled as in figure 5. Residual variances found for azimuths 0°, 90°, 180°, and 270° with the use of identity transformation as a model were 48.4 191.4, 50.3, and 216.4, respectively.

3.3.2 *Fits to lightness-condition data.* The results found in the lightness conditions are similar to those found in the color conditions. Figure 8 shows the averages of the residual mean squared errors in the 18 lightness conditions for the two observers, OR and MD. While the affine model fits the data best, the convergence model does nearly as well, in both the DKL (figure 8a) and the *LMS* (figure 8b) color spaces. As in the color conditions, no extra advantage of the general convergence model, with its six parameters, is found over the convergence model.
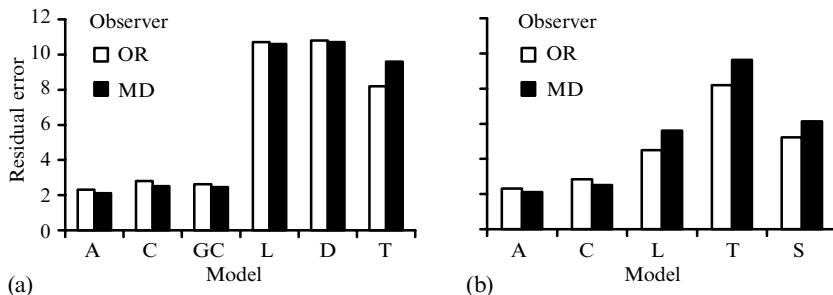

Figure 8. Model fits for the 18 lightness conditions, by observer. (a) Fits in the DKL color space. (b) Fits in the space of *LMS* cone excitations. Models are labeled as in figure 5. Residual variances found for observers OR and MD with the identity transformation used as a model were 1008 and 1137, respectively.

Figure 9 shows the quality of fits as a function of filter contrast reduction. Again, the contrast-reduction parameter of the convergence model is crucial to fitting the data. In the DKL color space (figure 9a), the error of the convergence model for filters with α equal to zero is 3.33, but is reduced to 2.19 when α is equal to 0.75. A similar decrease is found in the *LMS* color space (figure 9b).

Figure 10 shows the residual errors for the model fits as a function of filter color elevation. Note that the values found for the red filter with a target of convergence along the +LM half axis (elevation 90°) are larger than those found in the corresponding color conditions (see figure 7, azimuth 0°). This seeming discrepancy is due to the fact that the 15 reference colors used in the lightness conditions differ from the 17 reference colors used in the color conditions. In particular, the colors used in the lightness conditions spanned the three dimensions of color space and depend on the scaling of
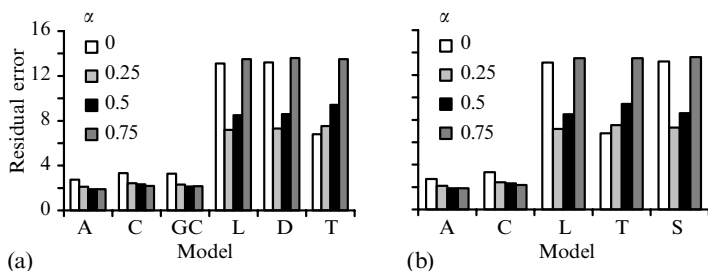
Figure 9. Model fits for the lightness conditions as a function of transparency contrast-reduction parameter α. (a) Fits in the DKL color space. (b) Fits in the space of *LMS* cone excitations. Models are labeled as in figure 5. Residual variances found for contrast-reduction values 0, 0.25, 0.5, and 0.75 with the identity transformation used as a model were 1055, 601.7, 900.1, and 1923, respectively.
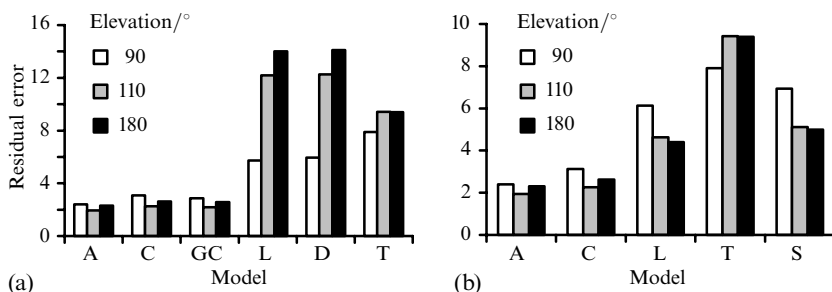

Figure 10. Model fits for the lightness conditions as a function of filter elevation. (a) Fits in the DKL color space. (b) Fits in the space of *LMS* cone excitations. Models are labeled as in figure 5. Residual variances found for elevations 90°, 110°, and 180° with the identity transformation used as a model were 363.3, 1279, and 1575, respectively.

the achromatic axis, in addition to the LM and S axes, while those used in the color conditions were confined to the equiluminous plane through the gray point G.

3.4 Fit parameters and filter parameters

The fits provided by the convergence model can be used to estimate the degree of color constancy exhibited by observers in these experiments. Table 4 shows for the color and lightness conditions the Pearson product moment correlation coefficients r that relate the fit contrast-reduction parameters to the filter parameters α. The correlation coefficients are uniformly high and range from 0.82 to 0.95. The best-fit lines have slopes that range from 0.44 to 0.69. These slopes quantify the degree of color constancy exhibited by observers in response to filter cloudiness (viz non-zero α): observers underestimate filter contrast reduction by a factor of nearly two.

We attempted to formulate similar estimates for color shift, but the results are less reliable. We compared the lengths, in the threshold-scaled DKL space, of the targets of convergence of the filters and the color shifts found in fits by the convergence

Table 4. Correlation between fit contrast-reduction parameters and filter α values for three observers' results in the color conditions and two observers' results in the lightness conditions. All of the correlations were highly significant.

	Observer				Observer	
	OR	MD	MW		OR	MD
Color				Lightness		
correlation	0.896	0.946	0.833	correlation	0.837	0.819
slope	0.446	0.686	0.663	slope	0.435	0.460

model to the data. As described in section 3.1.2, the achromatic, LM, and S axes were scaled so that one unit of distance along each axis would correspond approximately to threshold for detecting a stimulus along that axis.

Table 5 shows the correlation coefficients and the slopes that relate the vector lengths of the color shifts found in convergence-model fits to the vector lengths of the filters' targets of convergence. The correlation coefficients lie in the range 0.34 – 0.47 for the three observers in the color conditions. The correlation coefficients are somewhat higher at 0.69 and 0.74 for the two observers in the lightness conditions. With the exception of the correlation for observer MW in the color condition, these correlations are significant, if somewhat underwhelming. The best-fit lines have slopes in the range 0.38 – 0.56. These last numbers suggest that observers underestimate filter color shift by a factor of about two, which is about the same factor as for contrast reduction.

Table 5. Correlation between the lengths of fit color shifts and filter targets of convergence. In the color conditions, the results for observers OR and MD were significant at the 0.05 level, while those for observer MW were not. Both correlations in the lightness conditions were significant at the 0.01 level.

	Observer				Observer	
	OR	MD	MW		OR	MD
Color				Lightness		
correlation	0.47	0.452	0.34	correlation	0.737	0.685
slope	0.378	0.41	0.459	slope	0.557	0.542

4 Discussion

Observers can discount both shifts in color and changes in contrast when judging surface color and lightness. The results in figures 6 and 9, which show residual errors in model fits as a function of filter contrast-reduction parameter α, show clearly that a contrast-reduction parameter is needed to fit the color-matching data. It was Brown and MacLeod (1992) who documented our ability to discount changes in contrast. Our present work with the convergence model joins their findings to provide a more complete picture of human color constancy.

The estimates of how much of the physical reduction in contrast is taken into account by observers in these experiments range from 0.44 to 0.69 (see table 4): observers underestimate filter contrast reduction by about a factor of two. We also found, although the data are less reliable, that observers underestimate filter color shift by about a factor of two (see table 5).

It is instructive to compare these values to those found in earlier work for the degree of color constancy exhibited by observers. Brainard and colleagues (1997) estimated that the degree of color constancy in the experimental results of Arend and colleagues (1991), who worked with simulated changes in illumination, was about 0.25. Brainard and colleagues took great care to simulate natural viewing conditions in their own experiments and found a higher value of about 0.6. This last number is closer to our estimates of how much observers take into account change in contrast and color shift in displays with surfaces that appear to lie behind a transparent filter.

Our use of filters that are modeled in a manner identical to one of the models of visual processing that we wish to test seems flawed logically. Yet, note first that the present manipulations lead to the perception of transparency and, so, are of intrinsic interest. Note, second, that it need not have been the case that we take filter contrast reduction into account when judging surface color. Were our visual systems unable to take contrast variation into account, then translation and von Kries models would have done as well in fitting the data as the more general convergence and affine models.

Yet we have found convincing evidence that observers do take contrast variation into account when judging surface color. Note, finally, that using physical manipulations that match one's model is a time-honored procedure. From the work of Foster and Nascimento (1994), we know that daylight variations tend to leave invariant ratios of cone excitations received from surfaces. Using daylight illumination in color-constancy experiments is thus tantamount to using a physical model that matches the von Kries scaling model. In all of these situations, stronger tests of the various models require a wider range of physical manipulations.

A more general form of the convergence model has a separate contrast-reduction parameter for each of three axes in color space (eg achromatic, LM, and S). Not unexpectedly, such a generalized convergence model fits the current data just as well as the affine and convergence models. Yet we did not manipulate independently the simulated contrast-reduction parameters along various axes in color space in these experiments. Future work will show whether one can discount contrast reduction differently along different axes in color space, whether there are cardinal axes for such effects, and whether there are multiple, higher-order mechanisms sensitive to change in contrast (Krauskopf et al 1986; Zaidi and Halevy 1993; D'Zmura and Singer 1999).

Research on transparency stresses the importance of perceiving scission or laminar segmentation (Mausfeld 1998) between underlying surfaces and an overlaid phenomena, such as a transparent filter, a spotlight, shadow, or fog (D'Zmura et al 1997; Faul 1997; Chen and D'Zmura 1998; Hagedorn and D'Zmura 1999). We believe that understanding the conditions for scission to be perceived can help us to understand human color perception in complex, natural scenes.

Scission is a perceptual correlate of certain conditions for color constancy spelled out in earlier work (D'Zmura 1992). In that work, it was shown that viewing a set of surfaces under two or more light sources can provide sufficient information for a trichromatic visual system to recover surface and light source spectral descriptors. The correspondence of surfaces seen under the two light sources must be known for the recovery to be possible. Such correspondence is most easily perceived in cases where a change in illumination creates an edge, under which the boundaries of surfaces pass. The resulting X-junctions help give rise to perceptual scission, in which readily identifiable surfaces are seen under two or more lighting conditions. The suggestion of the computational theory for human vision is that trichromats should exhibit color constancy when surfaces are viewed under two or more lighting conditions and scission is perceived: the surfaces are identifiable across the lighting conditions so that the assumption of surface correspondence is met. Transparent color filters can also be used to change the chromatic conditions under which surfaces are viewed, and it was pointed out in the earlier work that surface and transparent filter spectral properties can be recovered under such circumstances. The experimental work reported here verifies that human observers exhibit color constancy in these situations identified earlier by theoretical analysis of physical models.

However, the proper study of transparency perception must be a perceptual one rather than one which focuses on a particular physical model (D'Zmura et al 1997). This claim is based on the results of experiments which showed that transparency perception is possible when using equiluminous color shifts. Equiluminous color shifts are not natural stimuli; they cannot be produced with physical filters or episcotisters. The argument that the study of perception is not the study of a particular physical apparatus applies more generally to the study of color constancy. Change in illumination is just one way in which surface viewing conditions can change physically. In addition to relying on a physical manipulation like changing illumination to steer research on color perception, we can use perceptual criteria like scission as helpful guides.

References

Arend L E, Reeves A, Schirillo J, Goldstein R, 1991 "Simultaneous color constancy: papers with diverse Munsell values" *Journal of the Optical Society of America A* **8** 661 – 672

Bäuml K H, 1999 "Simultaneous color constancy: how surface color perception varies with the illuminant" *Vision Research* **39** 1531 – 1550

Beck J, 1978 "Additive and subtractive color mixture in color transparency" *Perception & Psychophysics* **23** 265 – 267

Brainard D H, Brunt W A, Speigle J M, 1997 "Color constancy in the nearly natural image. 1. Asymmetric matches" *Journal of the Optical Society of America A* **14** 2091 – 2110

Brainard D H, Wandell B A, 1992 "Asymmetric color-matching: how color appearance depends on the illuminant" *Journal of the Optical Society of America A* **9** 1433 – 1448

Brown R O, MacLeod D I A, 1992 "Saturation and color constancy", in *Advances in Color Vision. Technical Digest* (Washington, DC: Optical Society of America) pp 110 – 111

Chen V J, D'Zmura M, 1998 "Test of a convergence model for color transparency perception" *Perception* **27** 595 – 608

Da Pos O, 1989 *Trasparenze* (Padua: Icone)

Derrington A M, Krauskopf J, Lennie P, 1984 "Chromatic mechanisms in lateral geniculate nucleus of macaque" *Journal of Physiology (London)* **357** 241 – 265

D'Zmura M, 1992 "Color constancy: surface color from changing illumination" *Journal of the Optical Society of America A* **9** 490 – 493

D'Zmura M, Colantoni P, Knoblauch K, Laget B, 1997 "Color transparency" *Perception* **26** 471 – 492

D'Zmura M, Rinner O, Gegenfurtner K R, 1998 "Color and lightness of a surface seen behind a transparent filter" *Perception* **27** Supplement, 170

D'Zmura M, Singer B, 1999 "Contrast gain control", in *Color Vision: From Genes to Perception*, Eds K R Gegenfurtner, L T Sharpe (Cambridge: Cambridge University Press)

Faul F, 1997 "Theoretische und experimentelle Untersuchung chromatischer Determinanten perzeptueller Transparenz", Dissertation, Christian-Albrechts-Universität, Kiel, Germany

Foley J D, Van Dam A, Feiner S K, Hughes J F, 1990 *Computer Graphics. Principles and Practice* 2nd edition (New York: Addison-Wesley)

Foster D H, Nascimento S M, 1994 "Relational colour constancy from invariant cone-excitation ratios" *Proceedings of the Royal Society of London, Series B* **257** 115 – 121

Gegenfurtner K R, 1992 "PRAXIS: Brent's algorithm for function minimization" *Behavioral Research Methods, Instruments and Computers* **24** 560 – 564

Gerbino W, Stultiens C I F H J, Troost J M, Weert C M M de, 1990 "Transparent layer constancy" *Journal of Experimental Psychology: Human Perception and Performance* **16** 3 – 20

Hagedorn J B, D'Zmura M, 1999 "Color appearance of surfaces viewed through fog" *Investigative Ophthalmology & Visual Science* **40**(4) S750

Krauskopf J, Williams D R, Mandler M B, Brown A M, 1986 "Higher-order color mechanisms" *Vision Research* **26** 23 – 32

Kries J von, 1905 "Die Gesichtsempfindungen", in *Handbuch der Physiologie des Menschen* volume 3, Ed. W Nagel (Braunschweig: Vieweg) pp 109 – 279

Lennie P, D'Zmura M, 1988 "Mechanisms of color vision" *Critical Reviews in Neurobiology* **3** 333 – 400

MacLeod D I A, Boynton R M, 1979 "Chromaticity diagram showing cone excitation by stimuli of equal luminance" *Journal of the Optical Society of America* **69** 1183 – 1186

Mausfeld R, 1998 "Colour perception: From Grassmann codes to a dual code for object and illuminant colors", in *Color Vision* Eds W Backhaus, R Kliegl, J Werner (Berlin: Walter de Gruyter) pp 219 – 250

Metelli F, 1974 "The perception of transparency" *Scientific American* **230**(4) 91 – 98

Smith V C, Pokorny J, 1975 "Spectral sensitivity of the foveal cone photopigments between 400 and 500 nm" *Vision Research* **15** 161 – 171

Wyszecki G, Stiles W S, 1982 *Color Science. Concepts and Methods, Quantitative Data and Formulae* (New York: John Wiley)

Zaidi Q, Halevy D, 1993 "Visual mechanisms that signal the direction of color changes" *Vision Research* **33** 1037 – 1051